JNC TN9400 2000-101

System Assessment and Calibrations of the Knudsen Effusion Quadrupole Mass Spectrometer

August 2000

OARAI ENGINEERING CENTER
JAPAN NUCLEAR CYCLE DEVELOPMENT INSTITUTE

本資料の全部または一部を複写・複製・転載する場合は、下記にお問い合わせください。

〒319-1184　茨城県那珂郡東海村村松4番地49
核燃料サイクル開発機構
技術展開部　技術協力課

Inquiries about copyright and reproduction should be addressed to:
Technical Cooperation Section,
Technology Management Division,
Japan Nuclear Cycle Development Institute
4-49 Muramatsu, Tokai-mura, Naka-gun, Ibaraki, 319-1184,
Japan

© 核燃料サイクル開発機構（Japan Nuclear Cycle Development Institute）
2000

System Assessment and Calibrations of the Knudsen Effusion Quadrupole Mass Spectrometer

Jintao HUANG*, Tomohiro FURUKAWA*

Abstract

A vapor pressure measurement instrument was set up by utilizing the "Microvision Plus (LM70)" quadrupole mass spectrometer combined with the Knudsen vapor effusion cell. The purpose of the vapor pressure measurement is to obtain reliable thermodynamic data of sodium-iron complex compounds. Then, the behaviors of these compounds in various environmental conditions can be investigated in detail for analysis of sodium-leak related accidents in fast breeder reactors (FBR). Therefore, the reliability of the measurement system is of great importance.

The following major procedures were made step by step.

(1) Vertical alignment arrangements

(2) Alignment of the ion mass in Q-mass analyzer

(3) "True" signal identification

(4) Noise reducing

(5) Determination of electron impact conditions

(6) Sensitivity improvement by adjusting parameters

(7) Temperature calibration

(8) Vapor pressure calibration

First, special attention was paid to the mechanical settlements, exploration of the parameters' effects, calibrations of temperature and pressure. Second, the vapor pressure measurement system was optimized for the specific requirements based on the extensive investigation in this study. Furthermore, it is confirmed that the measured pressures of the standard vapor species (silver and lead) are accurate. Finally, identical result can be reproduced in the same conditions so that the measurement system is believed to be reliable for the future researches.

---

* Structure Safety Engineering Group, Advanced Technology Division,
O-arai Engineering Center

クヌーセン流出四重極質量分析計のシステム評価と校正

黄　錦涛*、古川　智弘*

要旨

四重極質量分析計（Microvision Plus LM70）とクヌーセン・セルを組み合わせた蒸気圧測定装置が完成した。今後、この装置を用いて、ナトリウム-鉄複合化合物の信頼性のある熱力学データを取得し、高速増殖炉のナトリウム漏えい時の詳細な腐食機構解析を研究していくことを予定している。このためには、本装置構成によって得られるデータの信頼性を事前に評価しておくことが重要である。

そこで、以下の主要項目について測定、調査および校正等を行った。

(1) クヌーセンセル-質量分析部間の垂直軸合わせ

(2) 質量分析部の質量数測定校正

(3) 真シグナル識別

(4) ノイズ減少評価

(5) 電子衝撃エネルギーの決定

(6) パラメータ調整による感度改善

(7) 温度校正

(8) 蒸気圧校正

はじめに、重要項目である機械的な装置調整、各種パラメータの影響調査、そして温度および圧力校正を実施した。そして、これらの広範な調査結果に基づき、蒸気圧測定条件を最適化した。さらに、標準試料（Ag、Pb）を用いて蒸気圧を測定し、得られた結果が文献値と一致すること、ならびに同一条件下で複数回の測定を行い、その再現性を確認した。これらの結果から、ナトリウム-鉄複合酸化物の測定を進めるにあたって、本システムから信頼性のある蒸気圧測定結果を得られることが確認された。

＊　大洗工学センター、要素技術開発部、機器・構造安全工学 Gr.

Content

Figure captions

List of tables

1. Introduction

High temperature mass spectrometry combined with the Knudsen effusion cell is one of the most important methods to measure partial pressures of vapor species over condensed substances. Theoretical description of the principals in detail can be found in many fundamental textbooks, for example, "Chemistry of Inorganic Vapors" by Dr. Klaus Hilpert [1]. For the convenience of readers, however, a brief introduction of basic calculation formulas employed in this report is given here.

There are several steps to obtain thermodynamic information of the substance of interest, such as, the absolute partial vapor pressures of the species, enthalpy of sublimation, ...etc.

- Evaporating the condensed sample at high temperatures
- Identifying the vapor species by scanning the ions of particular masses
- Selection of proper electron impact energy and other parameters
- Measuring the intensity of the ions and their temperature dependencies
- Calculation of the thermodynamic data
- Evaluation of the results

The partial pressure of a specific vapor species in the Knudsen cell is calculated by Eq. (1):

$$P(Pa) = K_s \times \frac{I \times T}{\alpha \times \beta \times \sigma}, \quad \ldots\ldots(1)$$

where Ks is the proportional constant that should be determined by standard reference, I is the value of ion intensity measured by the Q-mass analyzer, T in Kelvin is the specimen temperature inside the K-cell, σ is the electron impact ionization cross section of the target ion in unit of 1E−16 cm^2, α is the isotope abundance of the target ion, β is the electron magnification factor usually in unit of one.

One simple but important point is the difference between the pressure inside the Knudsen cell and the pressure in the vacuum chamber. It is the former that we want to

obtain. The K-cell acts as a small chemical reactor in which desired chemical reactions occur. The molecular beam ejected from the orifice of the K-cell can be analyzed by the Q-mass. The Q-mass can determine the ion intensity in the ionization room with satisfied precision. However, it is unable to directly obtain the absolute value of vapor pressure in the K-cell. On the other hand, some default parameters given by the Q-mass code suppler may no longer fit for the present purpose. For example, the default electron impact energy is set to be 70 eV. This is so large that most of the inorganic vapor molecules must be broken into a group of ions and/or molecules with smaller masses. That will definitely produce obstacles for accurate quantity analysis of vapor pressures. Therefore, careful selection of Q-mass parameters and calibrations must be made. Then, it may become available to carry out accurate and reliable measurement of absolute vapor pressures in the Knudsen cell. Finally, the equilibrium states inside the K-cell can be successfully interpreted from the information carried by the molecular beam. In the present study, measurement method, ideal conditions and most of the important parameters have been determined.

2. Experimental equipments

List of main equipments used in the study:

(1) Q-mass:
Microvision Plus LM70 (Spectra International LLC)

(2) Ion detection methods:
Faraday Cup or Secondary Electron Multiplier (SEM)

(3) Knudsen cell:
made of Mo, Beam Molecular K-cell (Biemtron Co. Ltd.)

(4) Heating material: made of Ta

(5) Maximum temperature: 1250 °C

(6) Thermocouple: W-Re

(7) Vacuum system: 7.6×10^{-2} Pa (Q-mass operation limitation) ~ about 10^{-7} Pa (the best vacuum that the system can actually achieve)

2.1. Vacuum system

Q-mass ionization room and the Knudsen cell are all installed in a vacuum chamber. Vacuum as high as 1E–7 Pa can be obtained by a TMP and rotary pump in series as shown here. A baking system is also equipped with the system in order to remove gases adsorbed on the surface of the vacuum chamber.

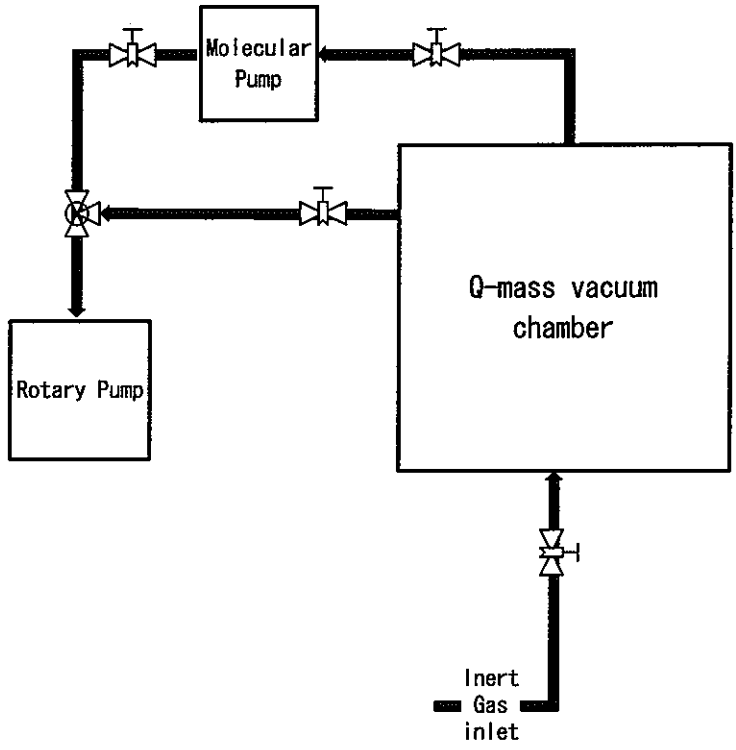

Fig. 1: Sketch of the vacuum system

2.2. Mechanical design of the Knudsen cell

The Knudsen cell is one of the most important parts in the system. A small orifice with diameter of 0.7mm was designed to guarantee that the effusion beam is in the molecular flow range. This parameter limits the highest partial vapor pressure that can be measured in the system. For example, Dr. Hilpert suggested $P(\max.) \approx 3.6/r$, i.e. about 10 Pa in the present case. Besides, an ideal cell should also have a uniform

temperature distribution and should be leak-free. Nearly 100% gas release should be the flow out of the orifice.

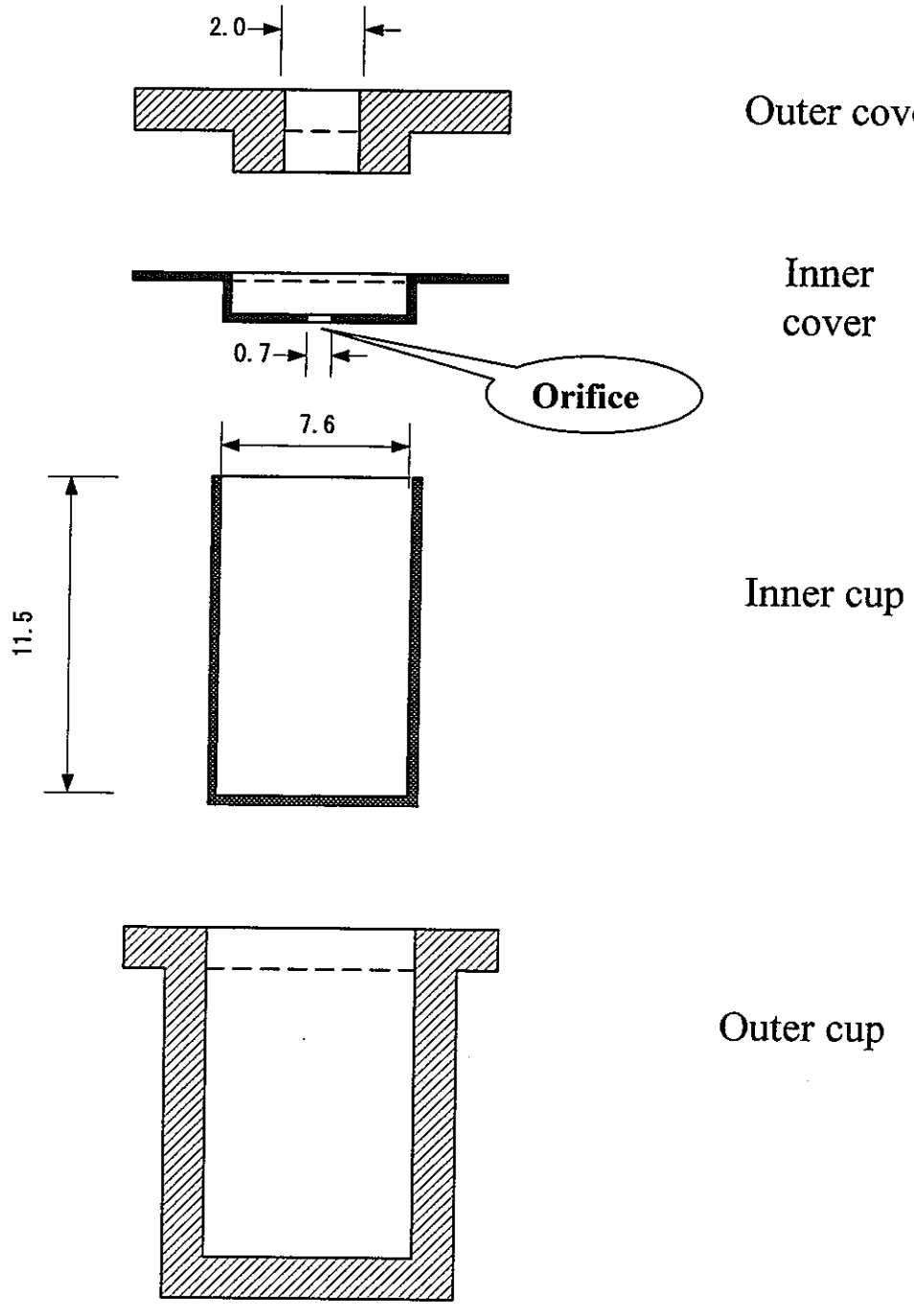

Fig. 2: Drawing of the Knudsen cell employed in the system

2.3. Arrangement of the measurement system

The geometric position of each part of the measurement system should be carefully fixed so that the molecular beam can just passing through the entrance center of the Q-mass ionization room. This is essential not only for higher detection efficiency, but also for better reproduction of measurements.

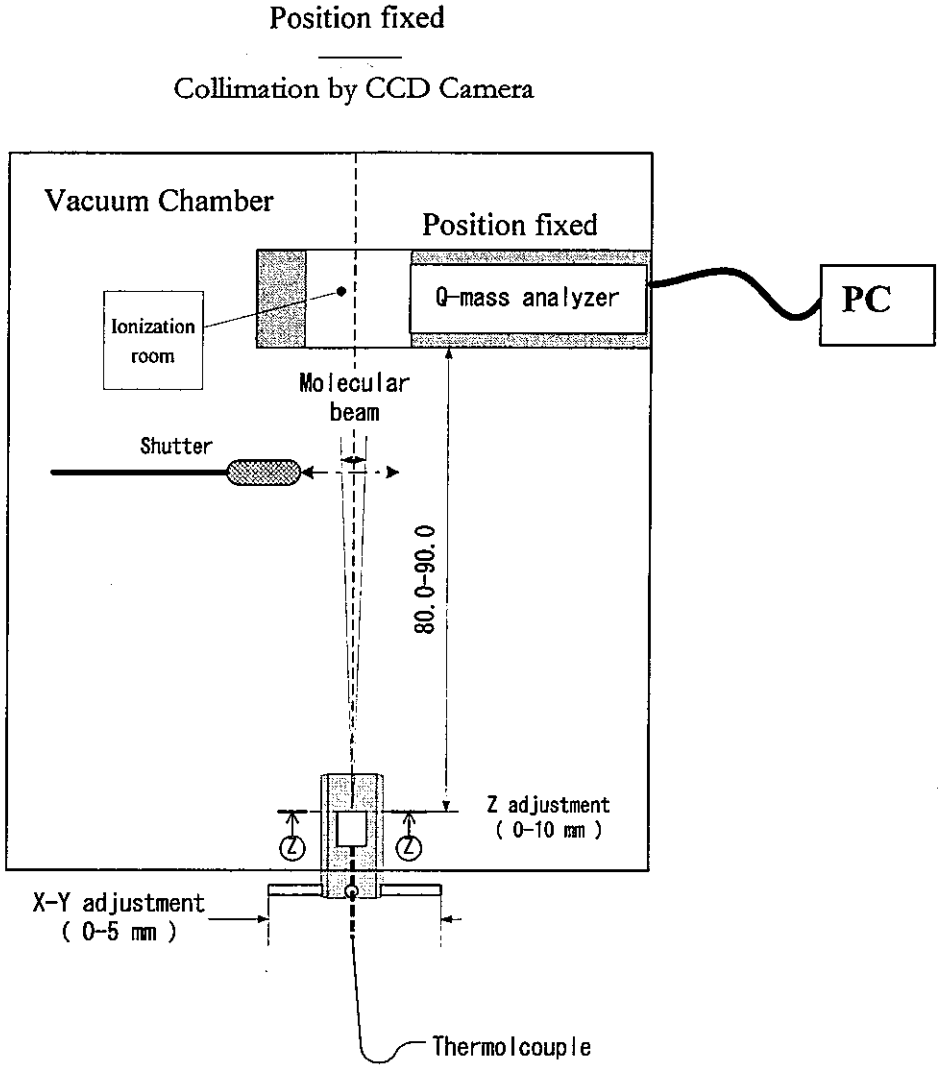

Fig. 3: Illustration of alignment settlement

The K-cell can be adjusted both horizontally (X-Y plane) and vertically (Z-axis). A CCD camera is equipped at the top of the system to confirm the status of axis adjustment. A typical top view is sketched in Fig. 4. A photograph (Fig. 5) taken by camera shows one successful example of arrangement.

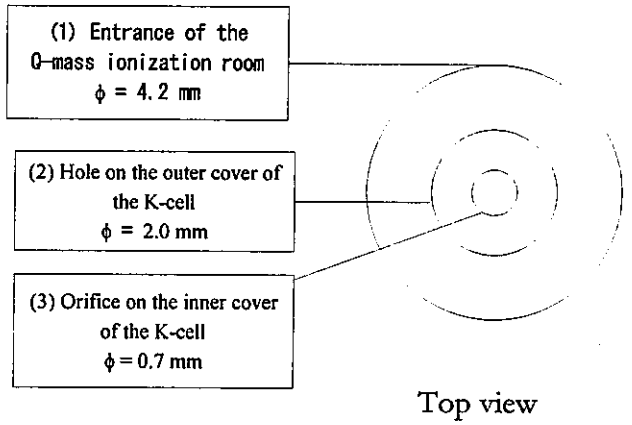

Fig. 4: Sketch of the top view of the system

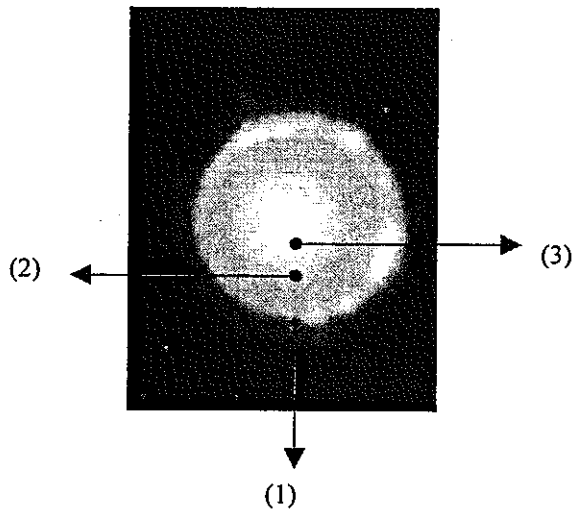

Fig. 5: Picture taken by a camera for the alignment conformation

Geometrical position of the K-cell:

Vertical position of the K-cell (Z-axis):	0 mm
Left (X-axis):	5.07 mm
Right (X-axis):	5.83 mm
Back (Y-axis):	5.08 mm
Front (Y-axis):	5.21 mm

3. Experimental results

3.1. Mass alignment

The default parameters have been set up by the RGA software as shown in Fig. 6. To get reliable data, however, it is essential to choose proper values according to our own tests. Therefore, the mass alignment was carried out as the following.

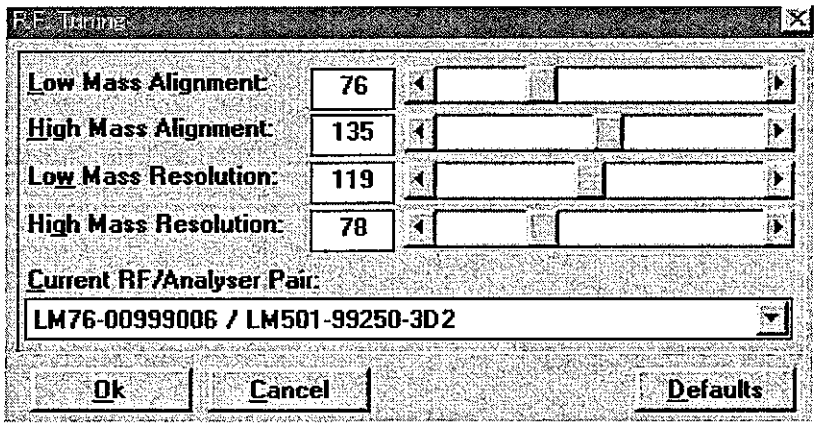

Fig. 6: Mass alignment adjustment menu

(1) High mass alignment

Using Ag as reference to calibrate those peaks with high atomic mass. It is not strange that the default value given by the computer code may not exactly match the real case as shown in Fig. 7-(A), where there was a position shift of about 0.5 atomic mass unit (amu) to the lower mass direction for both Ag^{107} and Ag^{109}. This small shift can cause dramatic error in practical measurement because the software automatically searches for the highest peak within ±0.3 amu of the requested mass. So attention should be paid to the high mass alignment because it may change from time to time. In this example, when the high mass parameter was adjusted from the default 135 to 148, the two peaks were reset to their correct positions as shown in Fig. 7-(B).

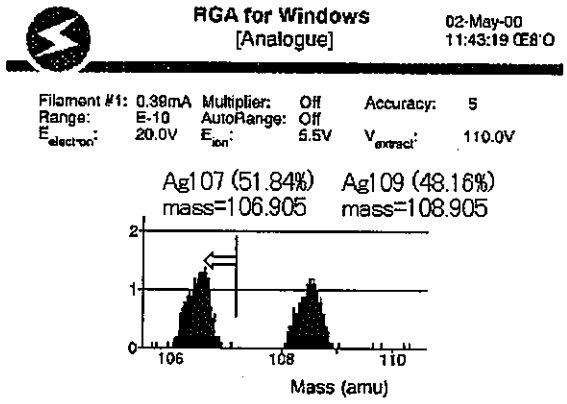

(A) Ag spectrum before mass alignment
High mass factor:135(default)

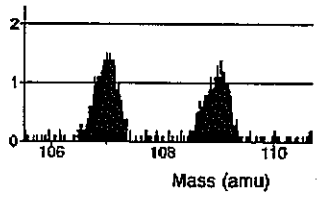

(B) Ag spectrum after mass aligment
High mass factor is set to 148

Fig. 7: High mass alignment result

(2) Low mass alignment

According to our own test, the Low Mass Alignment parameter needs scarce modification at all. So the default value is kept unchanged. However, the change of High Mass alignment parameter may also has a small influence on the low mass side as shown in Fig. 8. After the check, it can be seen that no large difference could be found.

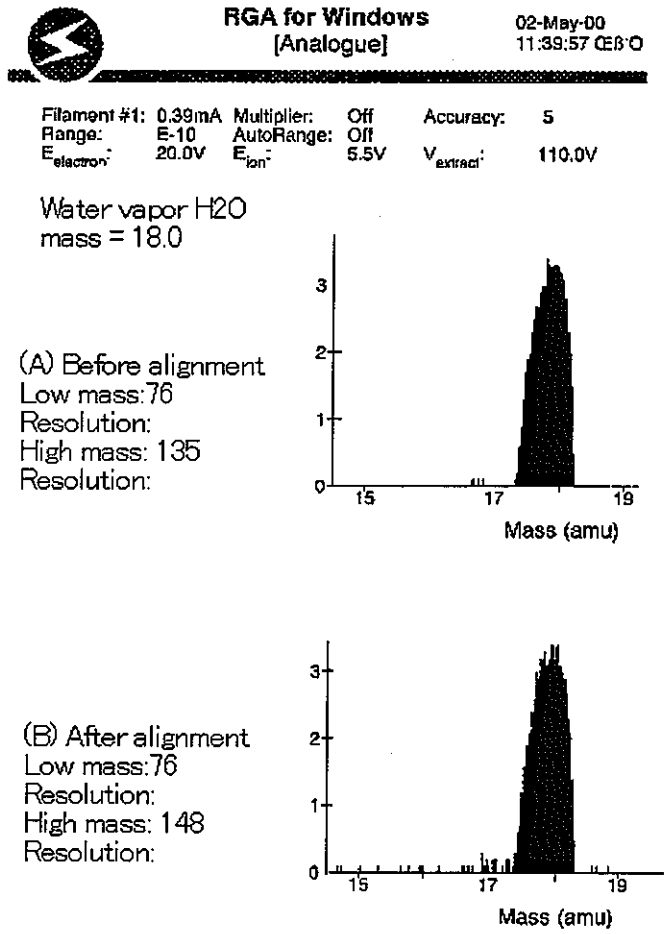

Fig. 8: Low mass alignment result

3.2. Precision investigation of the ion intensity measurement method

The intensity of ion with atomic mass N amu is automatically measured by the maximum height within N±0.3 amu. Thus, it is necessary to make sure if the peak height method is good enough for our application. For this purpose, the isotope abundance of silver was measured both by the peak height method and by the peak area method.

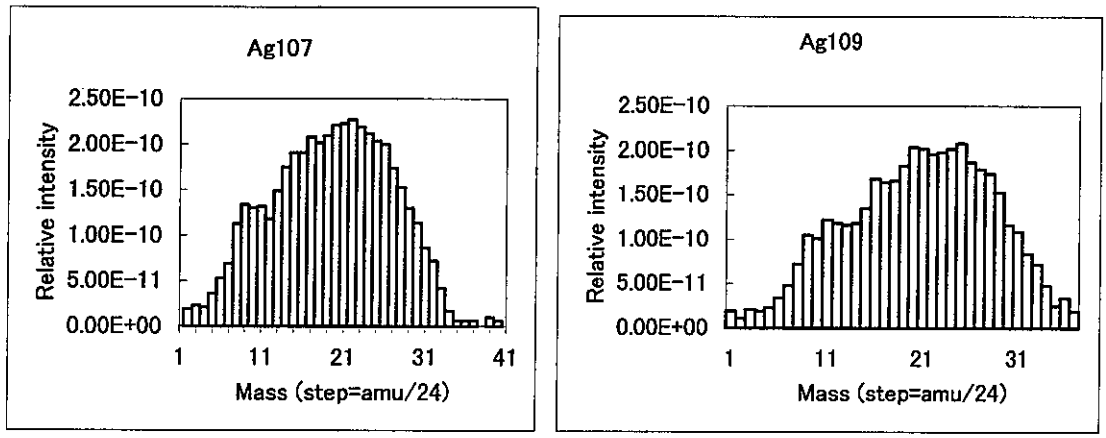

Fig. 9: Peak comparison of isotopes of silver. Ag ^{107} (left), Ag ^{109} (right)

Tab. 1: Comparison of peak intensity measurement methods

Measurement	Peak Area	Peak height	
Ag ^{107}	4.15E-09	2.27	
Ag^{109}	4.50E-09	2.04	
Calculation	Silver isotope abundance by Peak Area method	Silver isotope abundance by Peak Height method	Standard isotope abundance of the natural silver
Ag^{107}	52.02 %	52.67%	51.84% [Ref. 2]
Ag^{109}	47.98 %	47.33%	48.16 [Ref. 2]

The results show that both methods gave almost the same value that is consistent with the reference data. Generally speaking, measurement by peak height is faster and may cause relatively large error. From Table 1, its error is believed to be less than 1%. So, the default measurement method by peak height can be employed for further research works.

3.3. Ion detection sensitivity and setting of RF tuning parameters

There are four parameters that need to be determined as shown in Fig. 10.

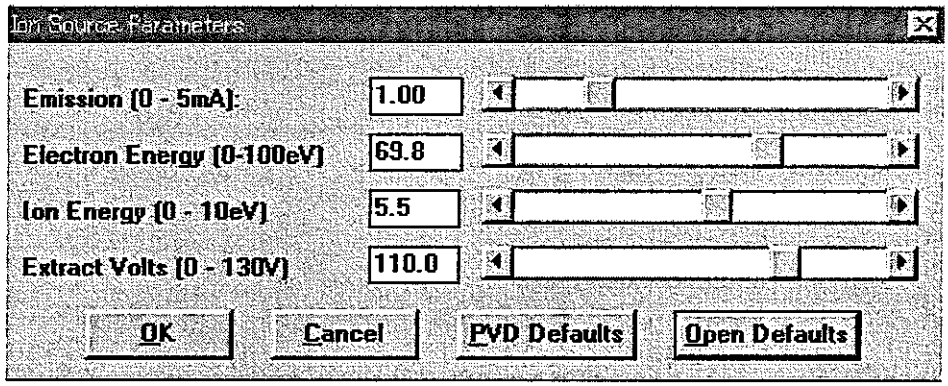

Fig. 10: RF tuning menu for setting Q-mass parameters

The ranges of the parameters are:

- Emission Current (E.C.): 0.00-5.00 mA
- Electron Energy (E.E.): 0.0-100.0 eV
- Ion energy range (I.E.): 0-10 eV
- Extract Volts (Ex. V.): 0-130 V

The energy of the impact electron is the first parameter that we should consider. "Ion Crack" or so-called "Molecular Fragmentation" would certainly happen for most of the vapor molecules if the default 70 eV were used. That may cause unnecessary confusing to identify the parent-child relationships. To avoid this kind of problem, the impact electron energy is usually set to be 10-20 eV[3]. On the other hand, low electron energy may limit the emission current. For example, the Emission current cannot be higher than 0.33 mA in the case of 20 eV electron energy because a safeguard will work to avoid any damage to the filament.

Ion energy and the extract voltages are the other two parameters that can affect detection efficiency of ions. They may be changed freely to obtain the best sensitivity for ion measurement. In Fig. 11, the effects of the two parameters were roughly explored.

Ideal area seems to be I.E.=4-8eV and Ex. V.=70-120V when E.E.=20 eV and E.C.=0.29 mA.

So, the default values, I.E.=5.5 eV and Ex.V.=110V, were employed in the measurements without any change.

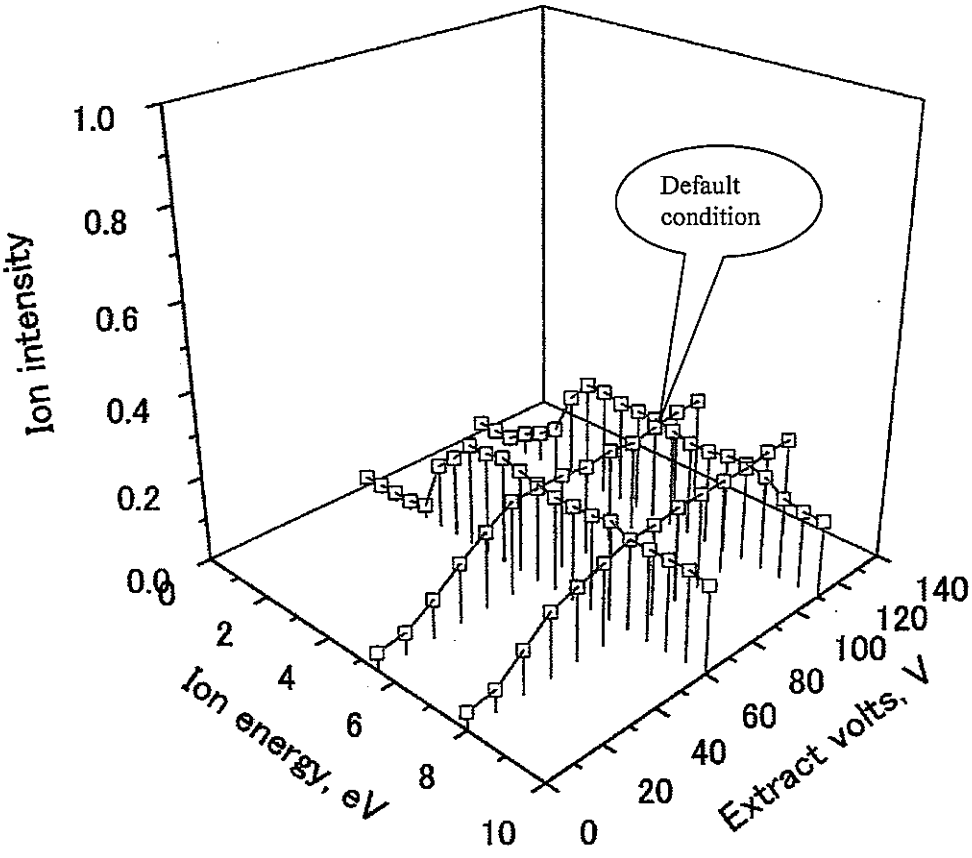

Fig. 11: Exploration of measurement sensitivity of ion intensity as functions of some of the Q-mass parameters

3.4. Noise reducing measure and its effects

An analysis of the noise spectrum in background shows that the main noise results from hydrogen (M=2), water vapor (M=18) and nitrogen (M=28) as shown in Fig. 12.

These background gases are usually adsorbed in the surface of the vessels made of stainless steel and may be released if the ambient temperature is increased.

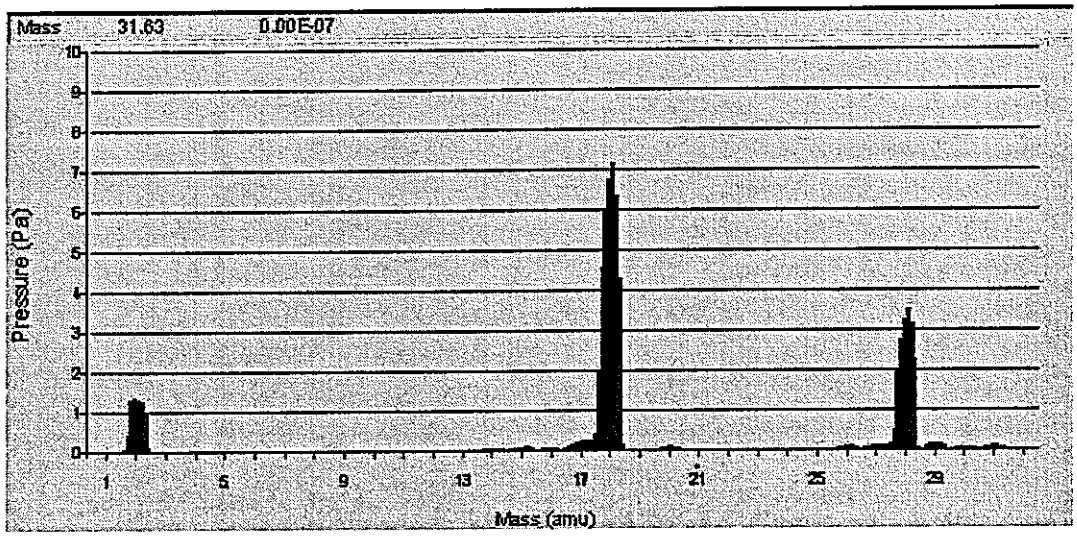

Fig. 12: The noise analysis result before liquid nitrogen is added to cool down the vacuum chamber

Liquid nitrogen is employed to cool down the center part of the vacuum chamber that surrounds the Knudsen cell. Its can dramatically decrease the level of background as shown in Fig. 13 compared to Fig. 12.

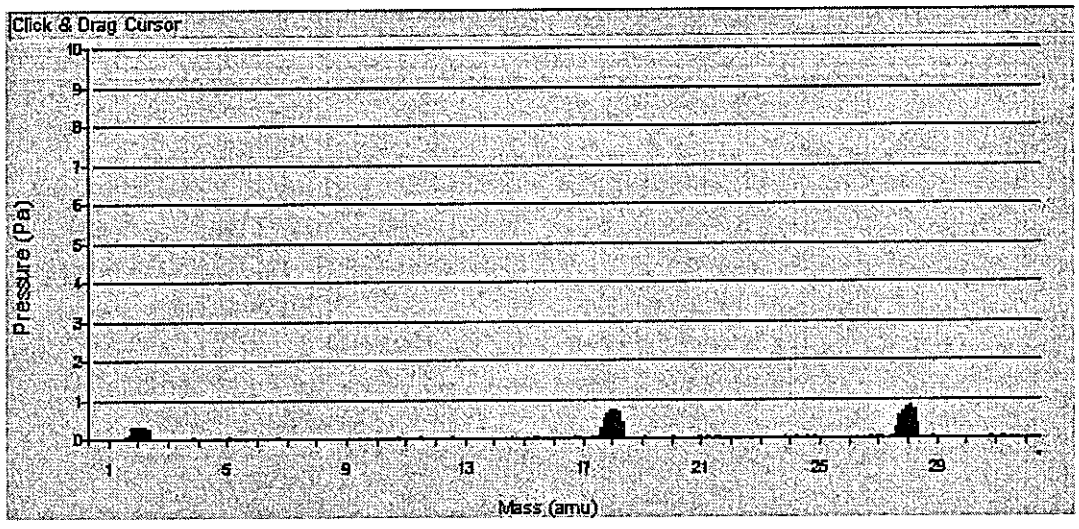

Fig. 13: The noise analysis result after liquid nitrogen is added to cool down the vacuum chamber

On the other hand, any possible influence on the true signal of sample must be investigated before normal measurements can be made. So, Ag^{107} and Ag^{109} were used to check if there is any influence on them when water vapor (mass=18) and nitrogen (mass=28) were tested simultaneously. As we expected, the true signals of Ag^{107} and Ag^{109} did not change even though the system was cooled down by liquid nitrogen as shown in Fig. 14 and Fig. 15. However, cooling down the system do has remarkable effect on reducing background, especially for water vapor. So, this treatment can be employed effectively and safely since it does not affect the true signals coming out of the K-cell.

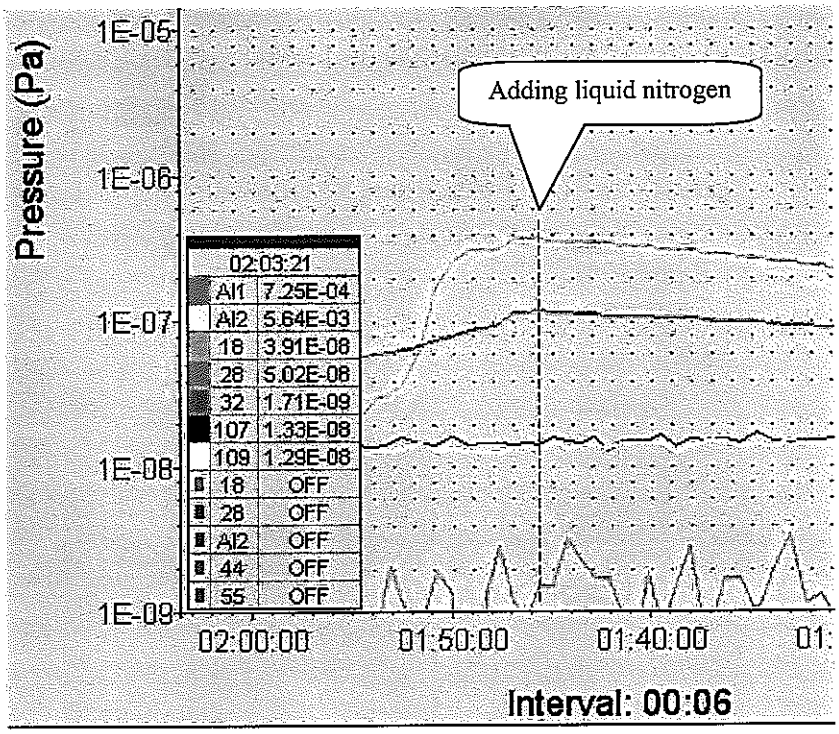

Fig. 14: Comparison of the influence of adding liquid nitrogen on background and the true signal Ag^{107} and Ag^{109}

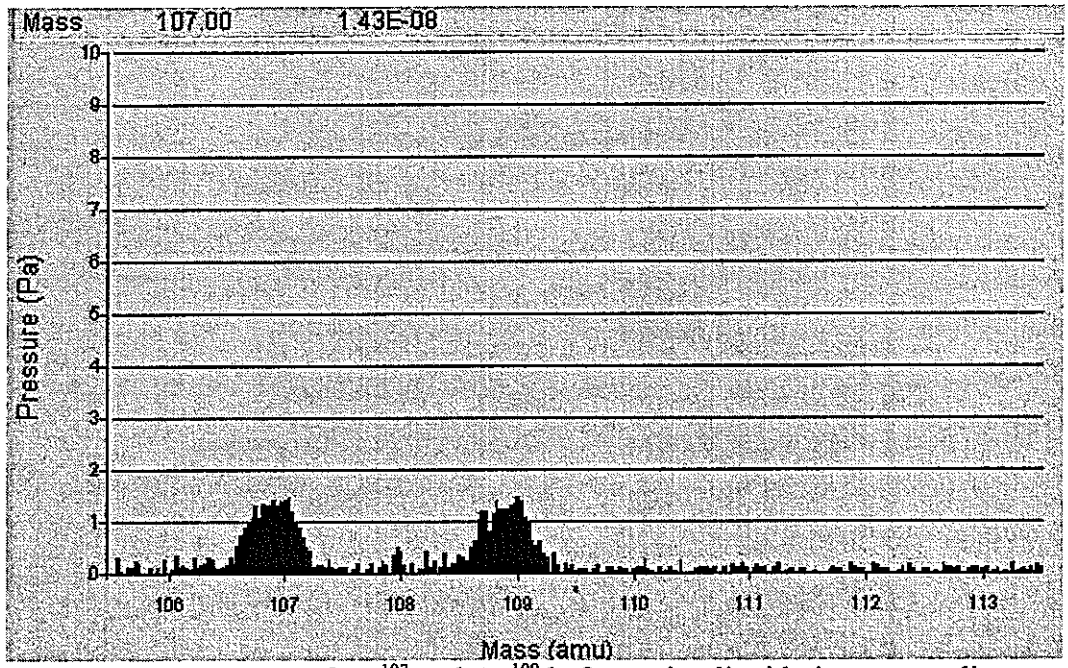

Fig. 15: Spectrum of Ag^{107} and Ag^{109} before using liquid nitrogen cooling

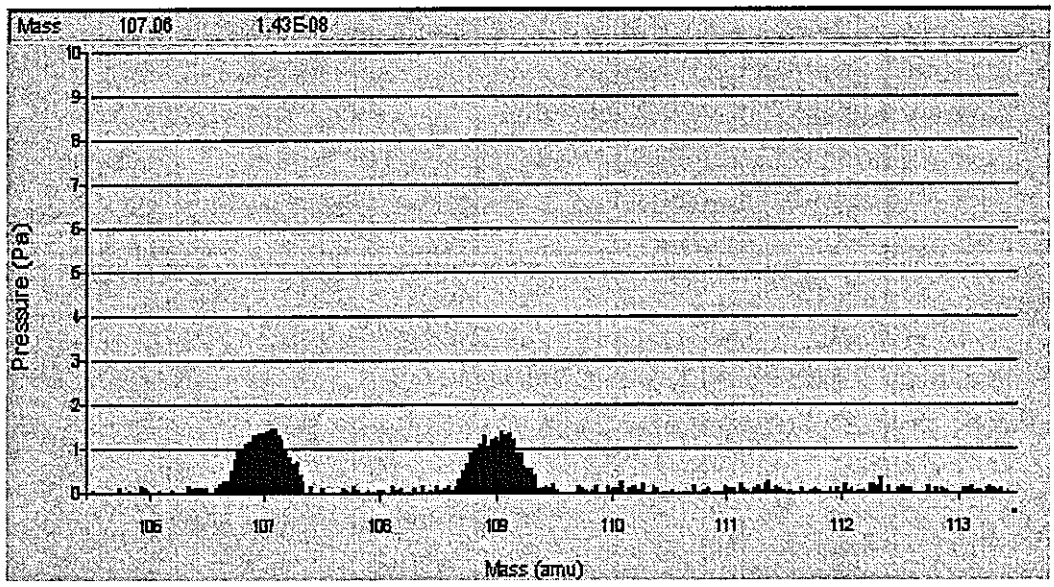

Fig. 16: Spectrum of Ag^{107} and Ag^{109} after using liquid nitrogen cooling

3.5. Ionization efficiency curve and electron energy check

Ionization efficiency curve (I.E.C.) is very important to know the ionization process of the target vapor atoms or molecules. From I.E.C, we can also understand the ionization potential of each vapor species. It will help us to determine proper value of impact electron energy.

The ionization efficiency curve of Ag^{107} was measured at Emission Current = 0.20 mA as shown in Fig. 17. It is clear that the ionization of silver atom is a typical simple ionization process, i.e., $Ag + e^- \rightarrow Ag^+ + 2e^-$. So, the impact electron energy was selected to be 20 eV in order to get highest sensitivity of silver ion detection.

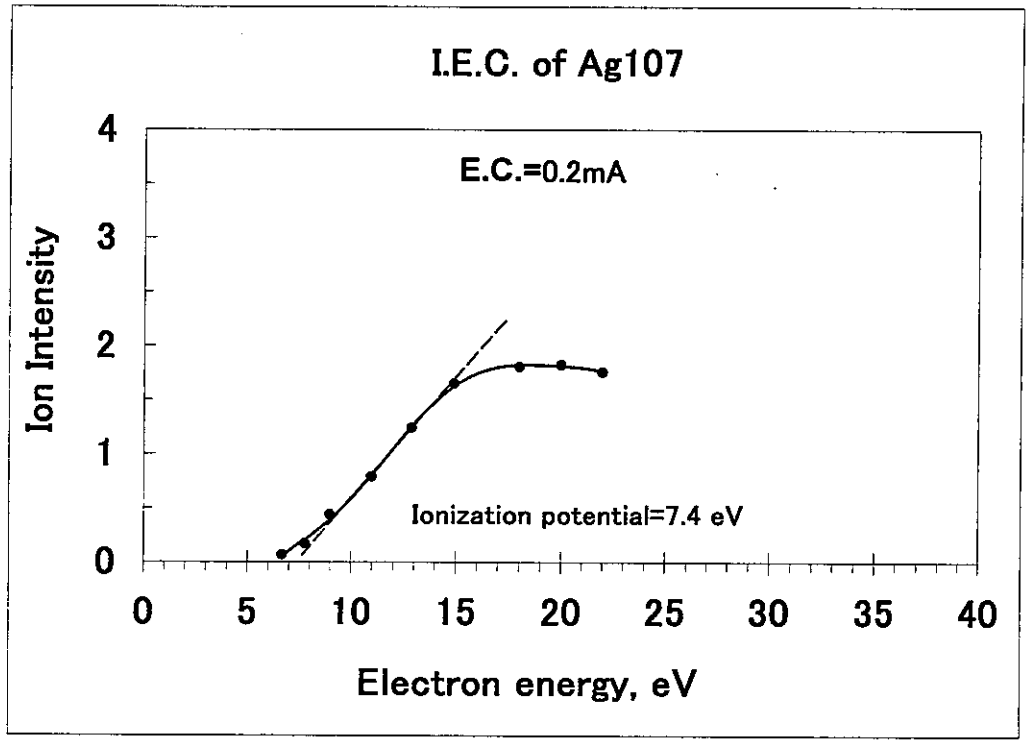

Fig. 17: Ionization efficiency curve of Ag^{107}

From the measurement, the ionization potential of silver is determined as about 7.4±0.5 eV. This is quite close to the 7.576 eV in reference[4]. It indicates that the energy

of impacting electrons is well controlled in the system so that it is reliable for our application.

3.6. Temperature calibration

Without doubt, sample temperature in the cell is different from the temperature measured outside of the cell because the thermocouple is connected to the outside of the K-cell as shown in Fig. 3. This problem must be solved before further thermodynamic treatment due to the importance of temperature. Relationship between the two temperatures is assumed to be close to linear,

$$T(\text{K-cell}) = a + b \times T(\text{set}). \quad (2)$$

Values of a and b are in need.

(1) Calibration by the melting point of silver

Silver can be used as a standard reference for temperature calibration because its melting point is well known. When heating the silver, for example, from 900 to 1000 °C in a proper speed, temperature change with time is recorded. At the melting point of Ag, a temporary temperature drop can be found due to the absorption of heat. It actually means the K-cell temperature will have a delay to follow the ambient temperature change. Similar phenomena could also be found for cooling down process. The measurement should be repeated many times so that any mistakes can be avoided. Therefore, the relationship between sample temperature and temperature measured outside of the Knudsen cell could be known.

$$\Delta T = T(\text{K-cell}) - T(\text{set}) \quad (3)$$

Measurement results:

The melting point (M.P.) of Ag in Mo cell is about 958.6°C, as shown in Ag-Mo phase diagram.

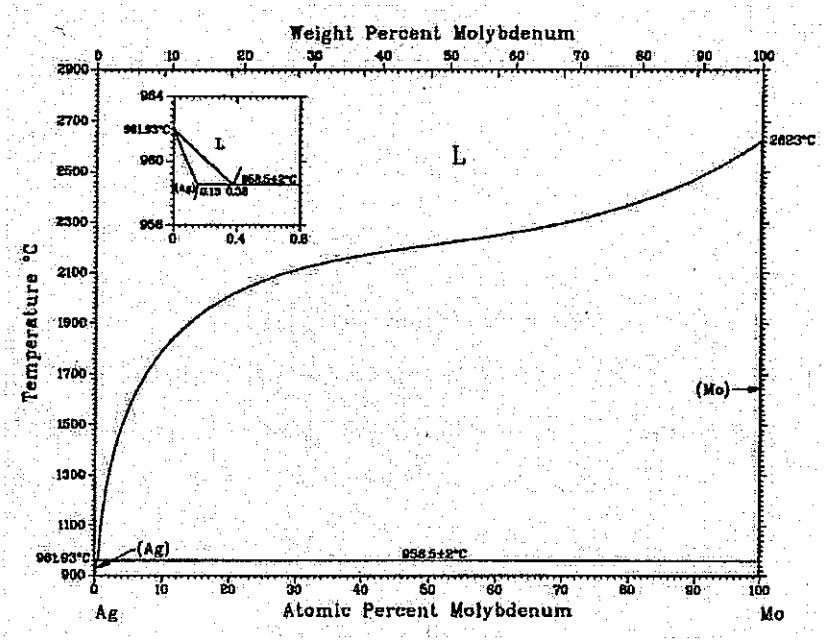

Fig. 18: Binary phase diagram of Ag-Mo

Tab. 2: Temperature measurement results by using silver as reference

Measurement Number	**Temperature Difference ΔT**
1	53*
2	49*
3	57
4	49
5	47
6	53
7	51*
8	47*
Final Result	$\Delta T = T$(K-cell)–T(set) $= 51 \pm 5$

Note: * the results gotten when decreasing temperature. The others were obtained when increasing temperature.

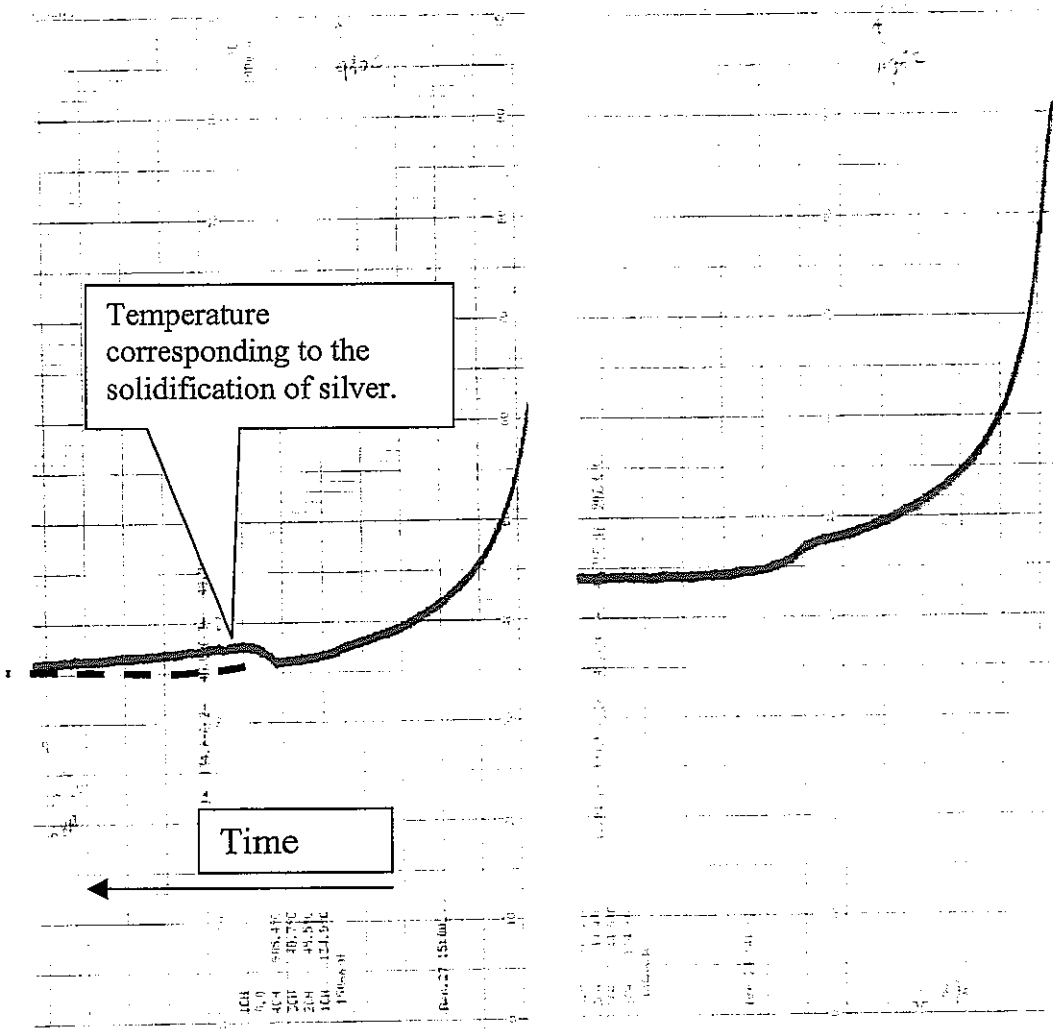

Fig. 19: The response delay of K-cell temperature when cooling down
(Left: No. 1; Right: No.2)

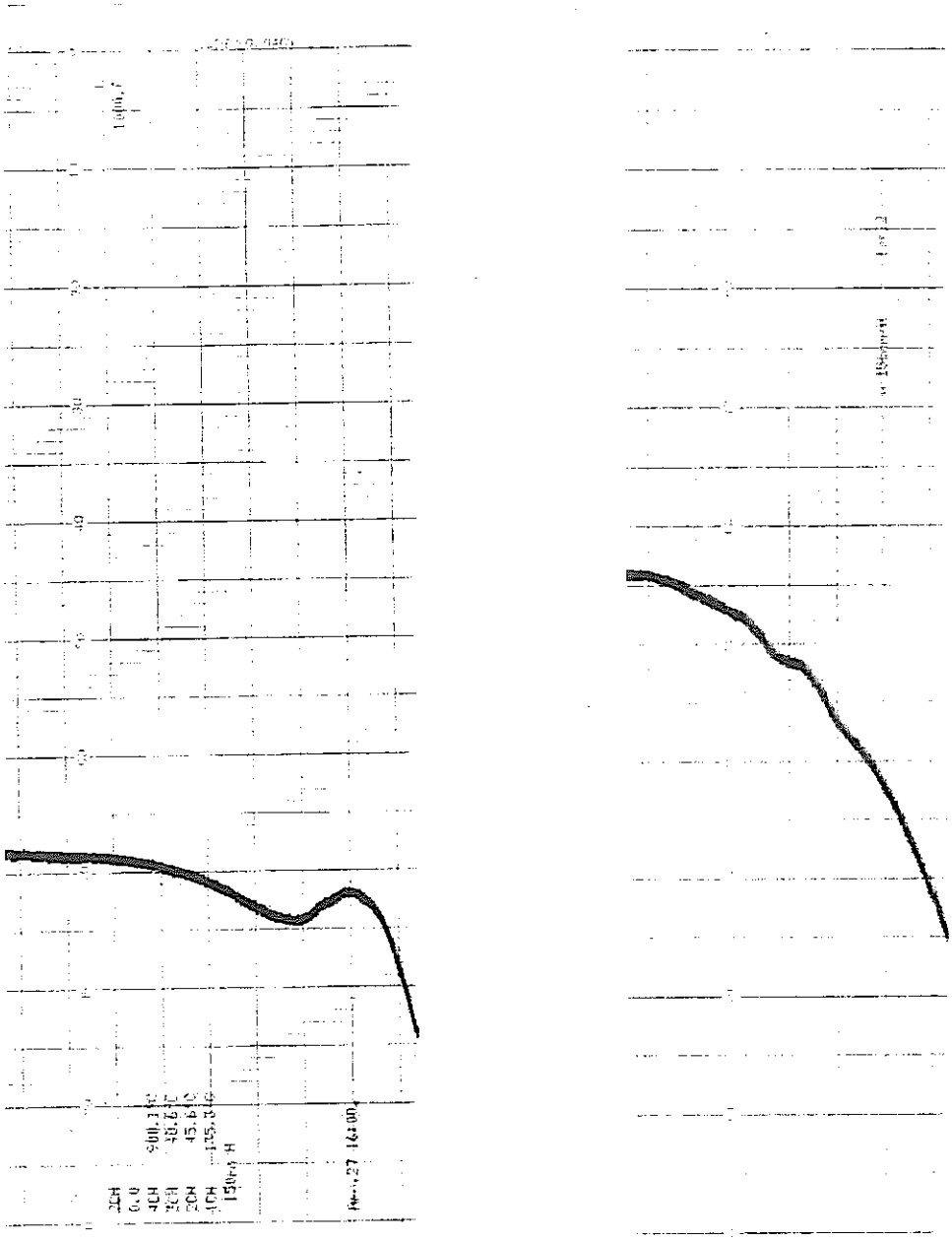

Fig. 20: The response delay of K-cell temperature when heating up

(Left: No. 3; Right: No.4)

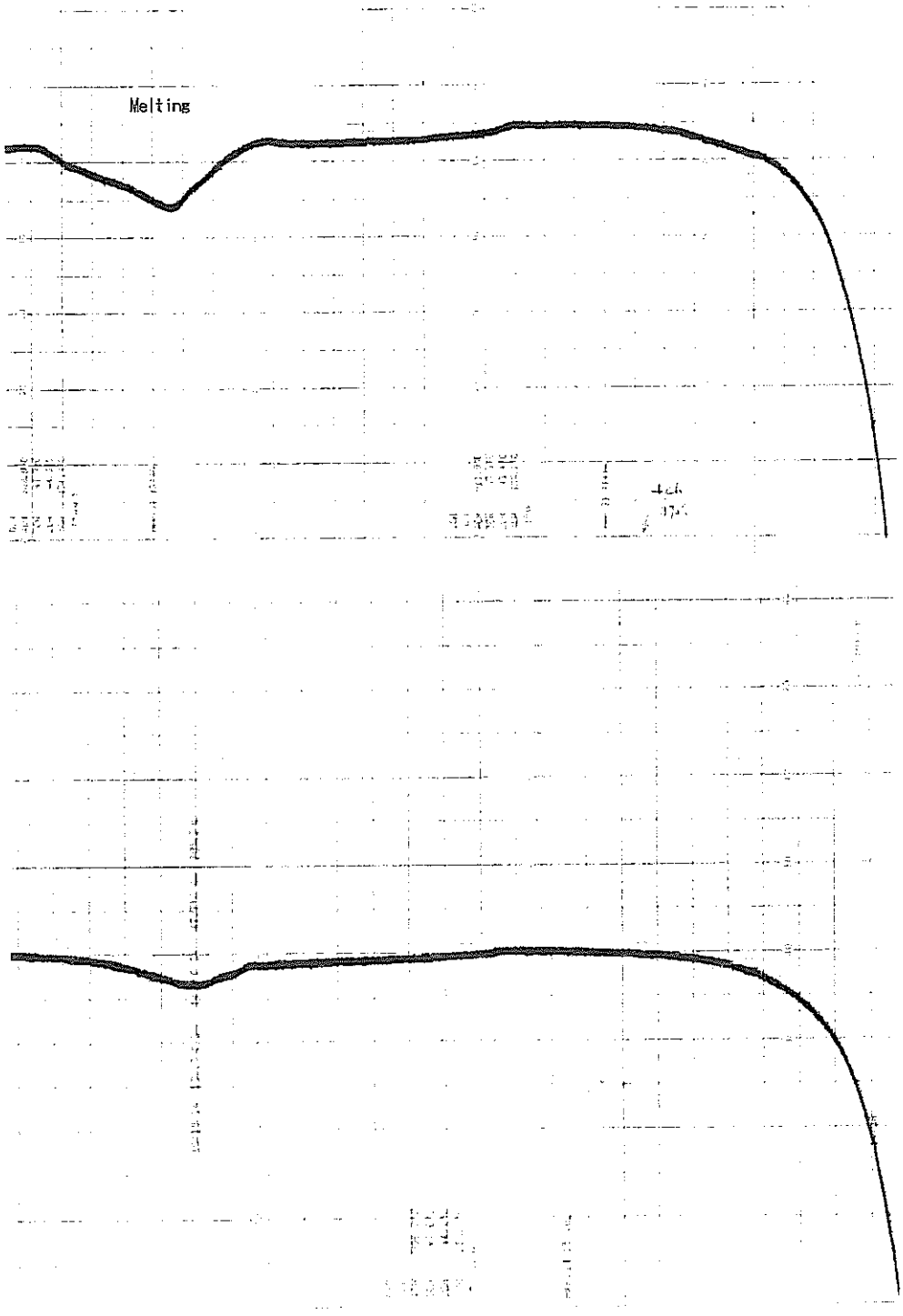

Fig. 21: The response delay of K-cell temperature when heating up

(Upper: No. 5; Lower: No.6)

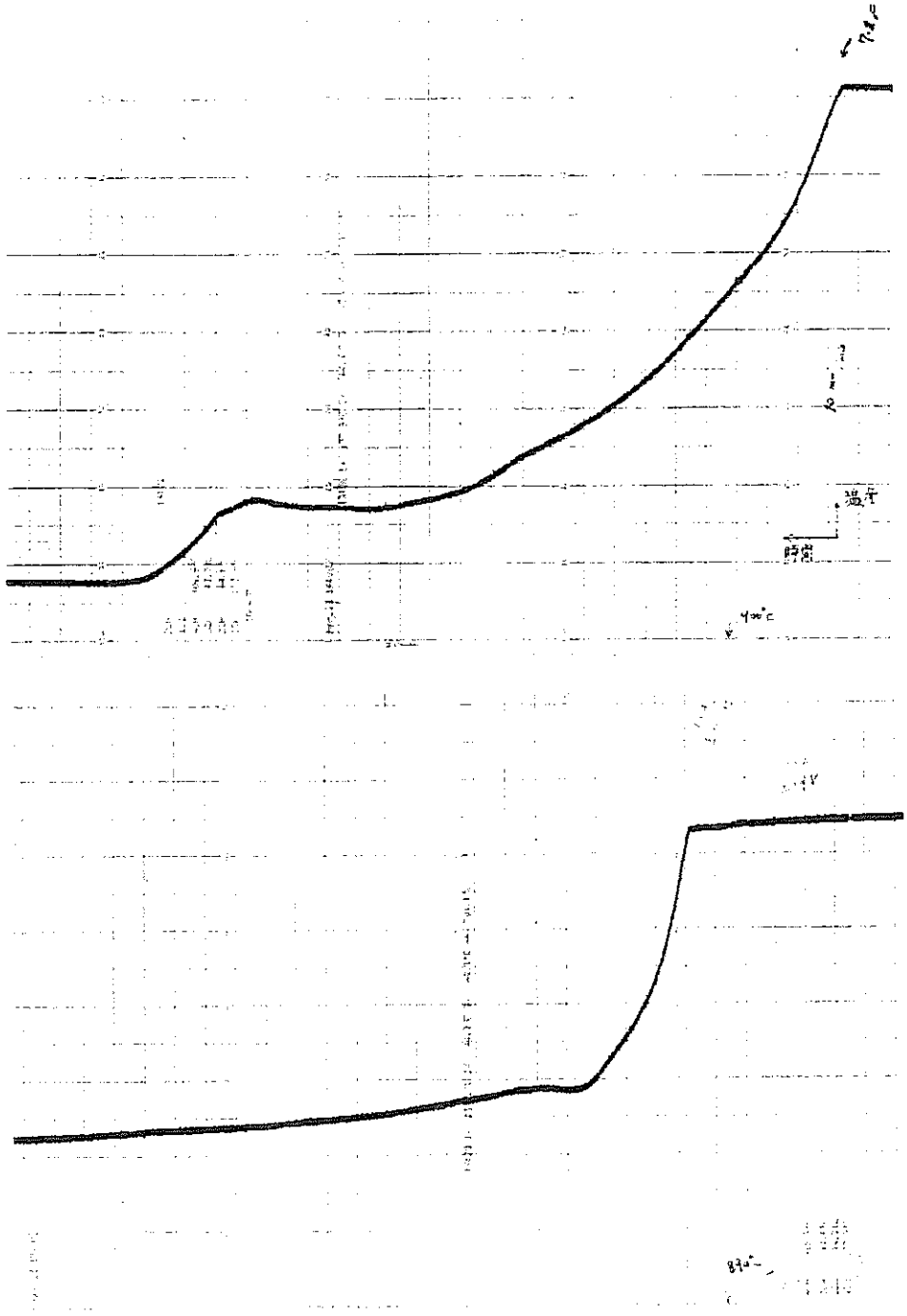

Fig. 22: The response delay of K-cell temperature when cooling down
(Upper: No. 7; Lower: No.8)

(2) Calibration by the melting point of lead

The melting point of Pb is about 327°C.

Tab. 3: Temperature measurement results by using lead as reference

Measurement Number	**Temperature Difference ΔT**
1	18
2	18
3	19
4	20
5	16
6	20
7	18
Final Result	$\Delta T = T$(K-cell)$-T$(set) $= 18 \pm 2$

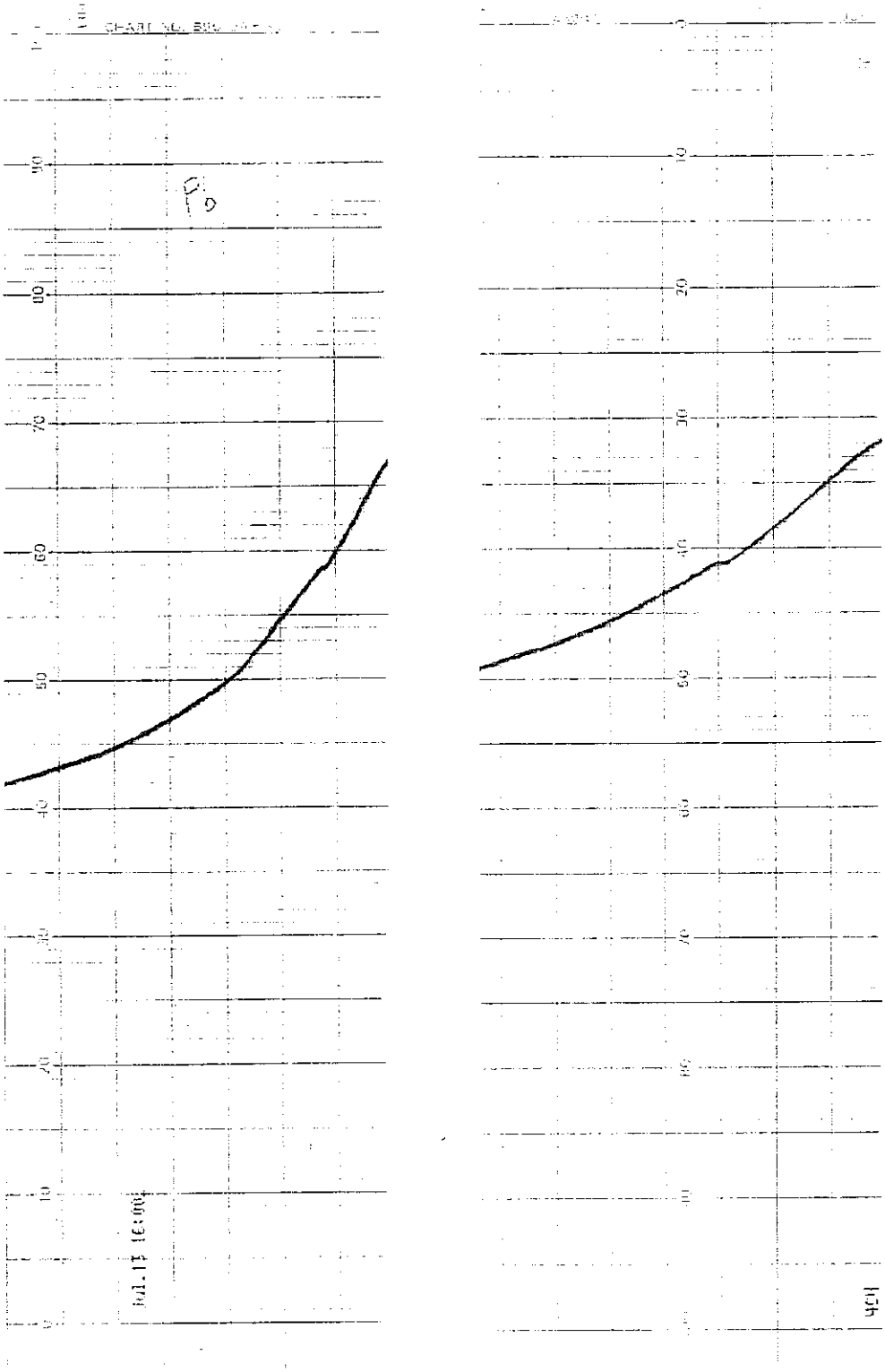

Fig. 23: The response delay of K-cell temperature when cooling down (No.1-2)

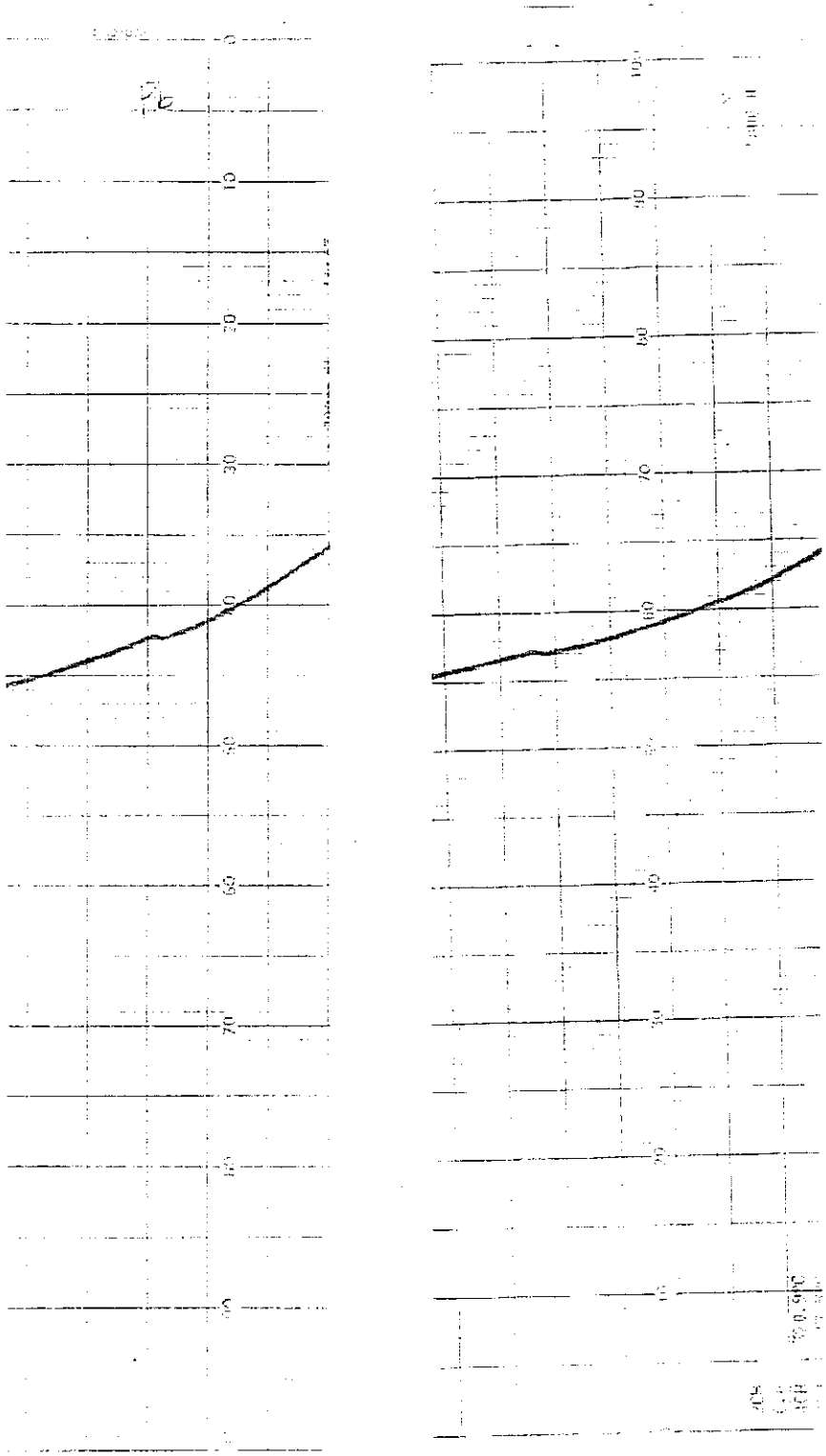

Fig. 24: The response delay of K-cell temperature when cooling down (No.3-4)

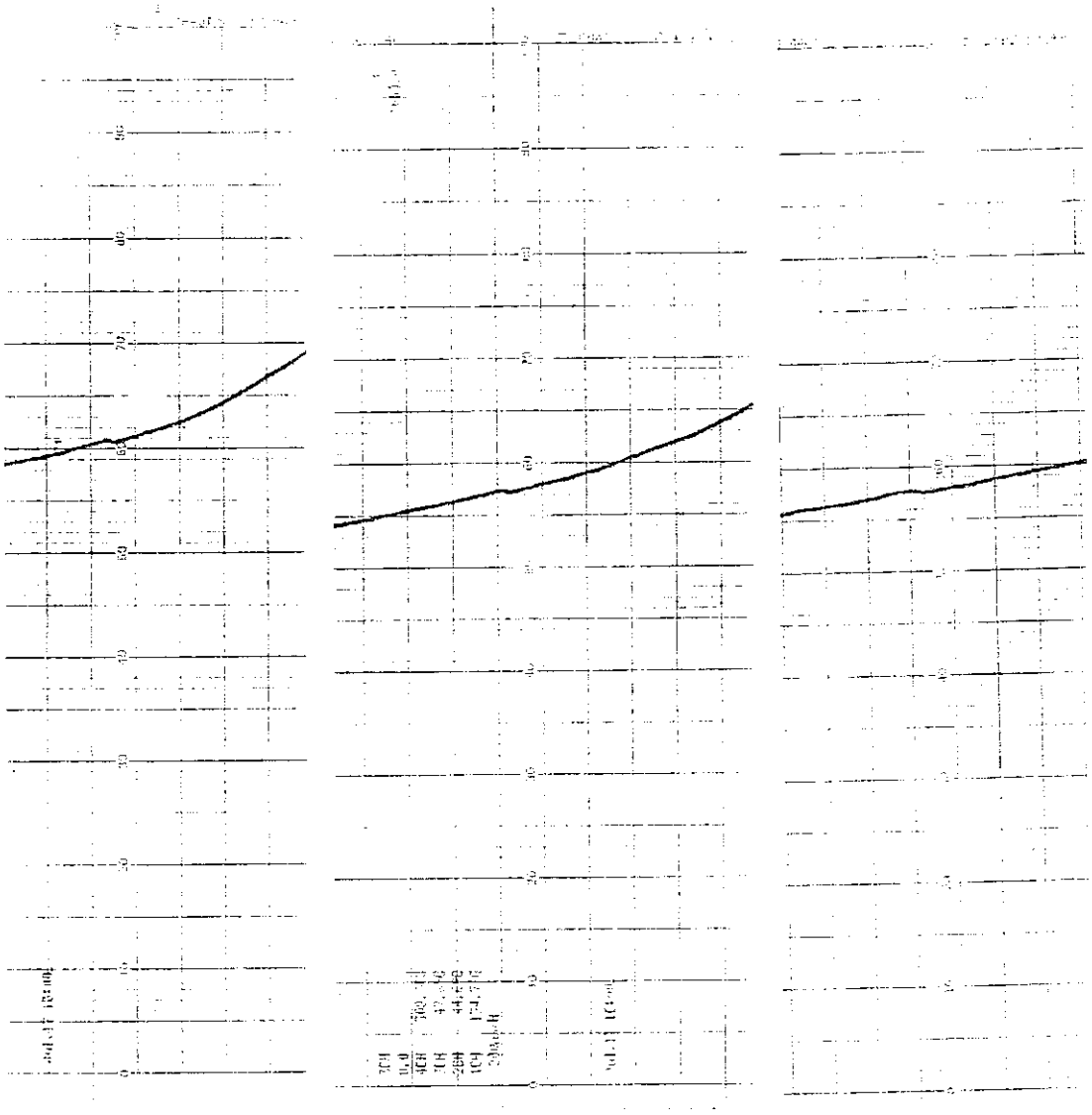

Fig. 25: The response delay of K-cell temperature when cooling down (No.5-7)

(3) Temperature calibration result

At room temperature, it is reasonable to assume no temperature difference between the Knudsen cell and the setup temperature. Thus, the temperature calibration formula can be expressed as Eq.(4):

$$T(\text{K-cell})\ ^{\circ}\text{C} = T(\text{set})\ ^{\circ}\text{C} \times 1.058 - 0.443 \qquad (4)$$

where T(K-cell) is the temperature inside the Knudsen cell while T(set) is the set-up temperature in the heating controller.

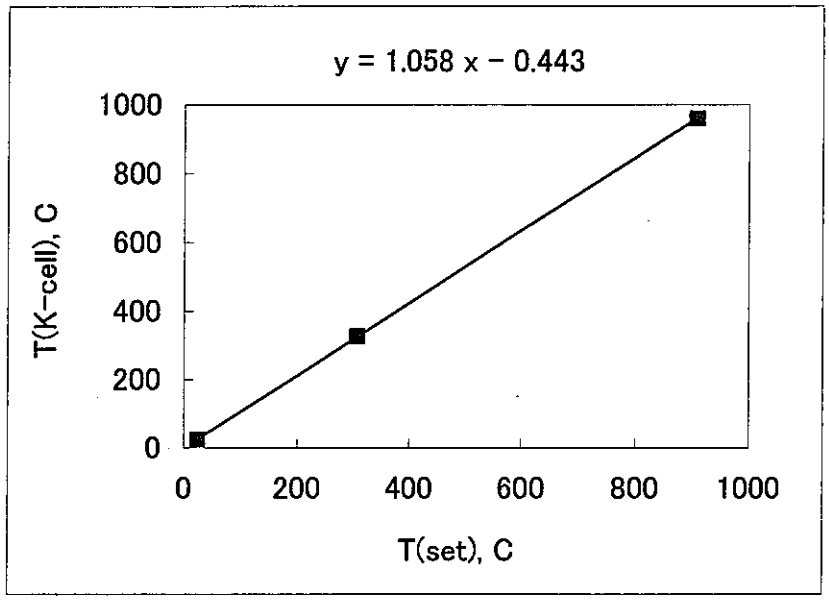

Fig. 26: Temperature calibration result

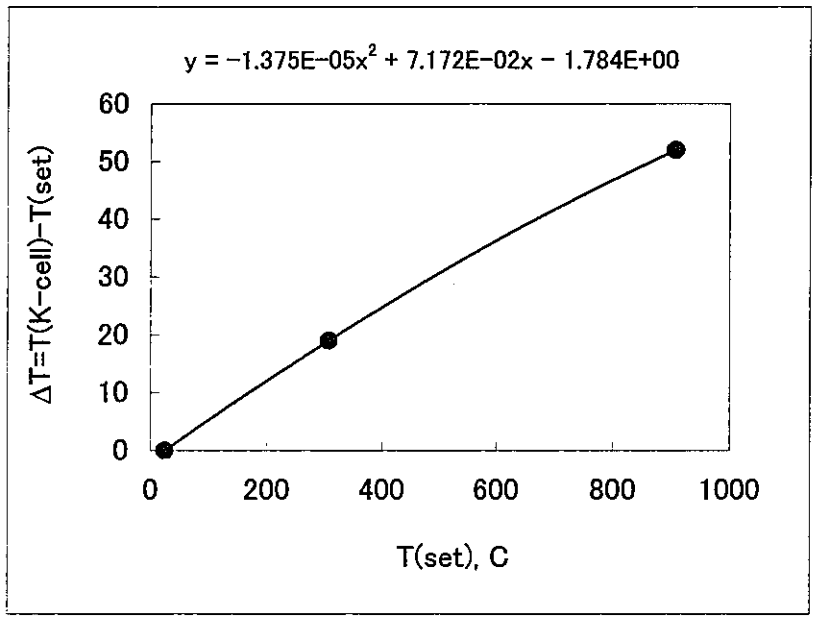

Fig. 27: Temperature difference as a function of set temperature

The conversation is also listed in Table 4 for convenience.

Tab. 4: Temperature conversion table for the K-cell

T(set), C	T(K-cell), C	T(K-cell), K	T(set), C	T(K-cell), C	T(K-cell), K
20	20.72	293.87	560	592.04	865.19
30	31.3	304.45	570	602.62	875.77
40	41.88	315.03	580	613.2	886.35
50	52.46	325.61	590	623.78	896.93
60	63.04	336.19	600	634.36	907.51
70	73.62	346.77	610	644.94	918.09
80	84.2	357.35	620	655.52	928.67
90	94.78	367.93	630	666.1	939.25
100	105.36	378.51	640	676.68	949.83
110	115.94	389.09	650	687.26	960.41
120	126.52	399.67	660	697.84	970.99
130	137.1	410.25	670	708.42	981.57
140	147.68	420.83	680	719	992.15
150	158.26	431.41	690	729.58	1002.73
160	168.84	441.99	700	740.16	1013.31
170	179.42	452.57	710	750.74	1023.89
180	190	463.15	720	761.32	1034.47
190	200.58	473.73	730	771.9	1045.05
200	211.16	484.31	740	782.48	1055.63
210	221.74	494.89	750	793.06	1066.21
220	232.32	505.47	760	803.64	1076.79
230	242.9	516.05	770	814.22	1087.37
240	253.48	526.63	780	824.8	1097.95
250	264.06	537.21	790	835.38	1108.53
260	274.64	547.79	800	845.96	1119.11
270	285.22	558.37	810	856.54	1129.69
280	295.8	568.95	820	867.12	1140.27
290	306.38	579.53	830	877.7	1150.85
300	316.96	590.11	840	888.28	1161.43
310	327.54	600.69	850	898.86	1172.01
320	338.12	611.27	860	909.44	1182.59
330	348.7	621.85	870	920.02	1193.17
340	359.28	632.43	880	930.6	1203.75
350	369.86	643.01	890	941.18	1214.33
360	380.44	653.59	900	951.76	1224.91
370	391.02	664.17	910	962.34	1235.49
380	401.6	674.75	920	972.92	1246.07
390	412.18	685.33	930	983.5	1256.65
400	422.76	695.91	940	994.08	1267.23
410	433.34	706.49	950	1004.66	1277.81
420	443.92	717.07	960	1015.24	1288.39
430	454.5	727.65	970	1025.82	1298.97
440	465.08	738.23	980	1036.4	1309.55
450	475.66	748.81	990	1046.98	1320.13
460	486.24	759.39	1000	1057.56	1330.71
470	496.82	769.97	1010	1068.14	1341.29
480	507.4	780.55	1020	1078.72	1351.87
490	517.98	791.13	1030	1089.3	1362.45
500	528.56	801.71	1040	1099.88	1373.03
510	539.14	812.29	1050	1110.46	1383.61
520	549.72	822.87	1060	1121.04	1394.19
530	560.3	833.45	1070	1131.62	1404.77
540	570.88	844.03	1080	1142.2	1415.35
550	581.46	854.61	1090	1152.78	1425.93
			1100	1163.36	1436.51

3.7. Ionization cross section as a function of electron impact energy

The electron impact ionization cross section of each vapor species is very important factor to obtain its corresponding pressure as expressed in Eq. (1). For most of the atomic ion such as silver and lead, their ionization cross-sections have been well studied so that the data given in reference were used [5].

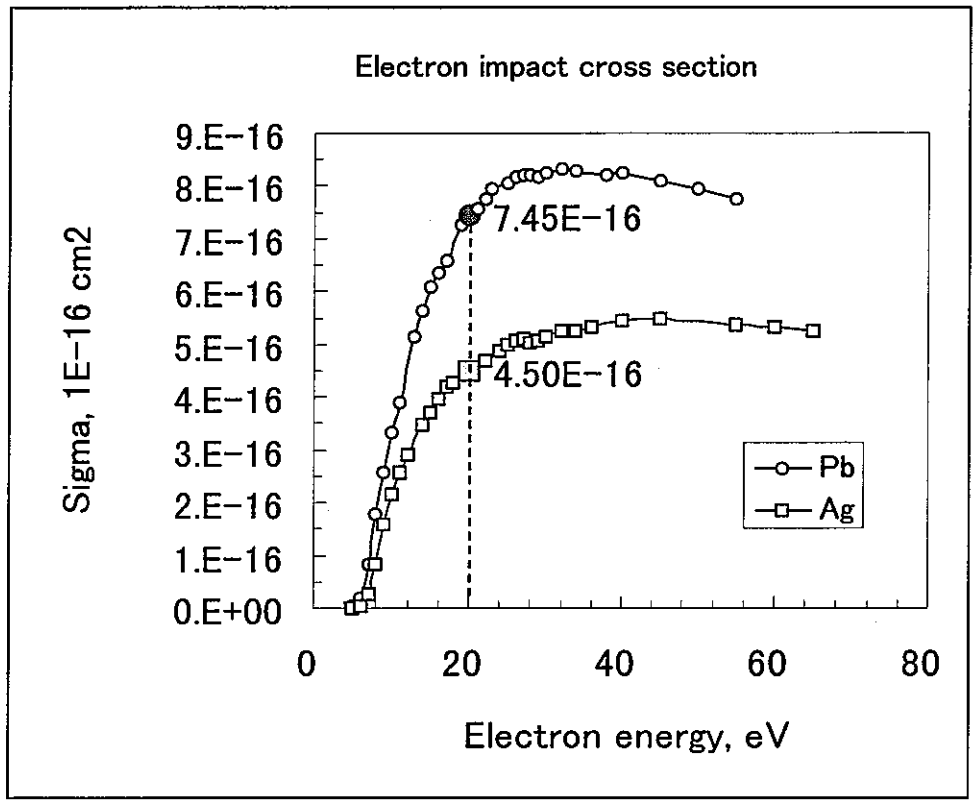

Fig. 28: Electron impact ionization cross sections of Ag and Pb

When the electron energy is set to 20 eV, the cross section of Ag and Pb are:

- Ag: 4.5 E–16 cm^2
- Pb: 7.45E–16 cm^2

3.8. Pressure calibration

Finally, pressure calibration, the most important procedure, can be done since all the other parameters have been determined. Once more, silver and lead are used as the references.

(1) Using Ag^{107} as standard reference

$$Ag(s,l)=Ag(gas) \quad (5)$$

$$\Delta G = = \Delta H - T\Delta S = - RT\, ln\, P(Ag) \quad (6)$$

In Table 5, the standard thermodynamic data from Thermo-Calc computer code[6] are listed. So, a comparison with the measurement result can be made.

Tab. 5: Enthalpy of vaporization of Ag(liq.)=Ag(gas)

T(K)	P(Pa)	$\Delta H/R$	ΔH (kJ/mol)	Average ΔH
1250	4.9673E–01			
1300	1.3300E+00	–32008	–266	
1350	3.3031E+00	–31931	–265	–265 kJ/mol
1400	7.6722E+00	–31855	–265	–63.45 kcal/mol

Note: Melting point: 1234K

Fig. 28 shows the temperature dependence of ion intensity of Ag^{107} when silver is turned into liquid over 1250 K. From the slope of curve log (I*T)-1/T, the enthalpy of vaporization can be calculated by the 2nd law treatment as follows,

$$\Delta H = (-31347 \pm 2289) \times 8.314 \text{ J/mol}$$

$$= -260.6 \pm 19 \text{ kJ/mol}$$

$$= -62.3 \text{ kcal/mol}$$

It is quite close to the theoretical result given in Table 5.

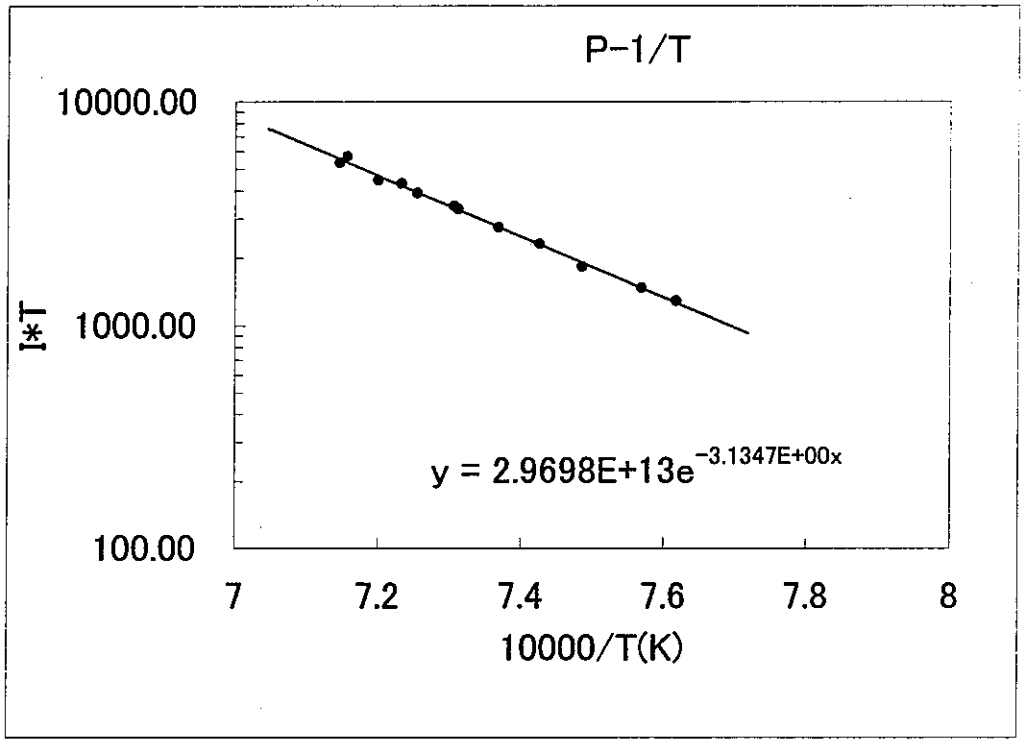

Fig. 29: Temperature dependence of the ion intensity of Ag^{107} over Ag(liq.)

Measurements were made at two separated times. First, the data were gotten when increasing temperatures (marked in circle). The second were obtained when decreasing temperatures (marked in triangle). They are in good consistent as shown later in Fig. 32.

(2) Using Pb^{208} as standard reference

Similar test was also made by using lead as reference. Since the temperature range is different from that of silver. This test is significant for a little lower temperature range.

$$\text{Pb(liq.)=Pb(gas)} \tag{7}$$

$$\Delta G = = \Delta H - T\Delta S = - RT \ln P(\text{Pb}) \tag{8}$$

The standard thermodynamic data obtained from Thermo-Calc computer code is given in Table 6.

Tab. 6: Enthalpy of vaporization of Pb(liq.)=Pb(gas)

T(K)	*P*(Pa)	Δ*H*/*R*	ΔH (kJ/mol)	Average ΔH
900	0.137708			
950	0.506532	−22272	−185.2	
1000	1.63114	−22219	−184.7	−185.4 kJ/mol
1050	4.74274	−22414	−186.4	−44.3kcal/mol

Note: Melting point: 602K.

In Fig. 30, two measurement results of temperature dependence of Pb^{205} are compared. So it is quite confident to conclude the reproduction is good enough in the present system.

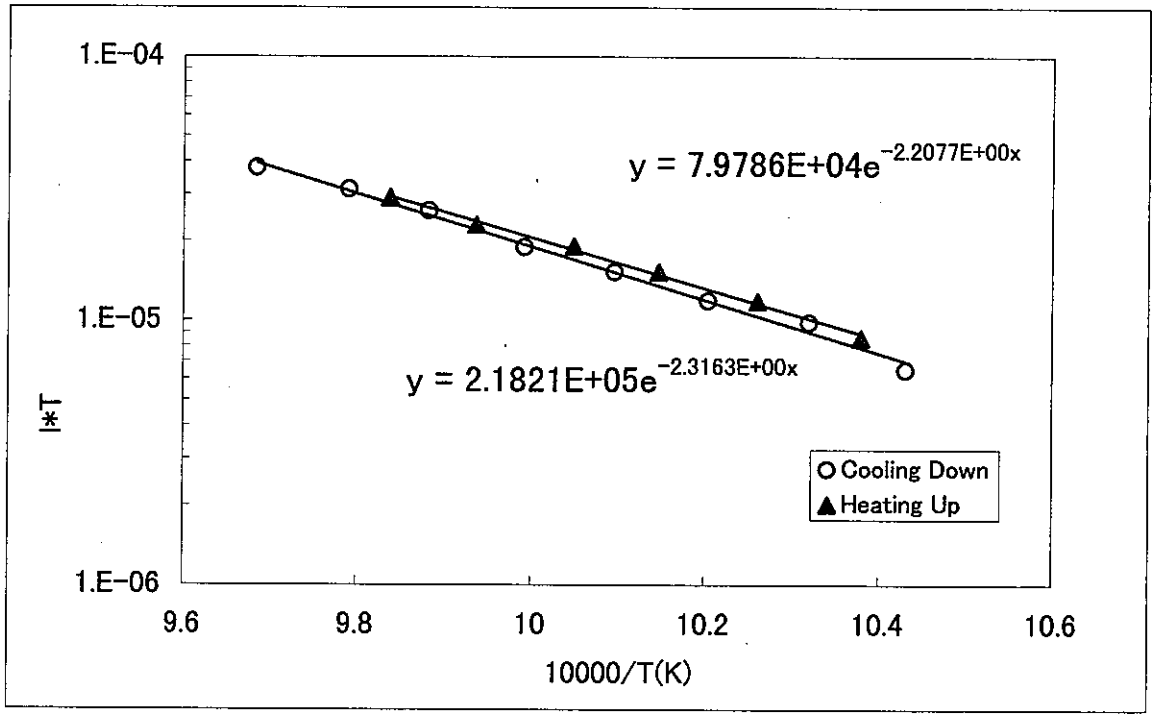

Fig. 30: The temperature dependence of ion intensity of Pb^{205} over Pb(liq.)

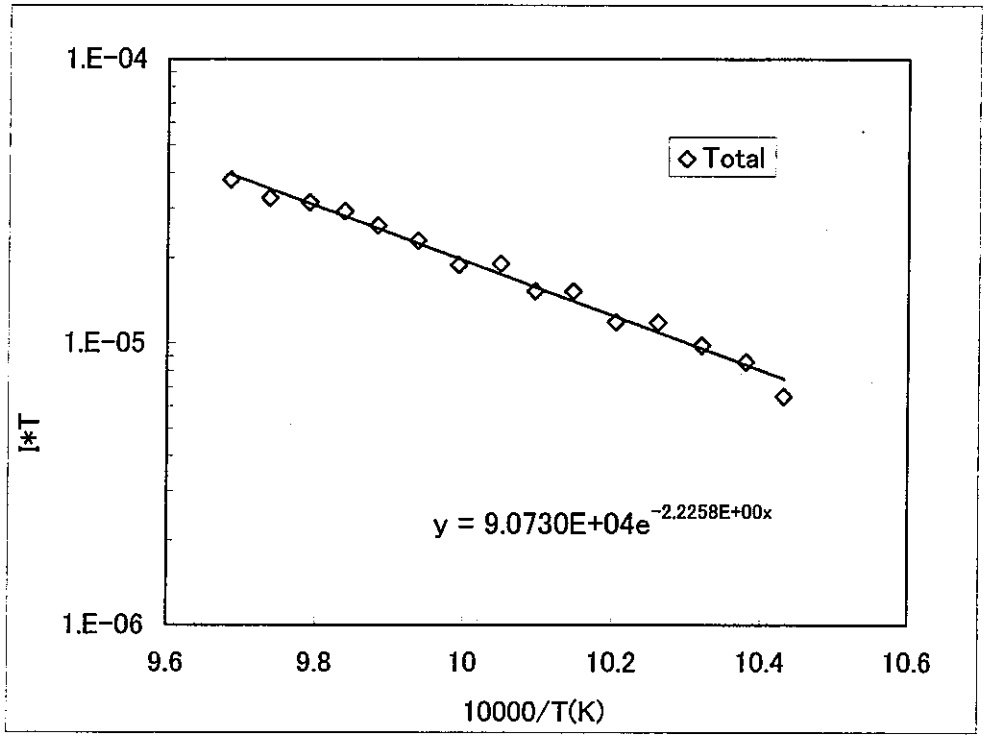

Fig. 31: Enthalpy of vaporization of Pb(liq.)=Pb(gas)

To obtain the average value of enthalpy of vaporization, all the two measurement data were used as shown in Fig. 31. From the measurement,

$\Delta H = -22258 \times 8.314$ J/mol

$= -185.0$ kJ/mol

$= -44.2$ kcal/mol

It agrees well with the theoretical result given in Table 6.

(3) Proportional constant at the optimized condition of measurement

The equilibrium pressure of Ag(gas) over Ag(liq.) can be expressed according to Ref.[7]:

$$\lg(P/\text{bar}) = -14709/T - 1.53 \lg(T) + 11.229 \qquad (9)$$

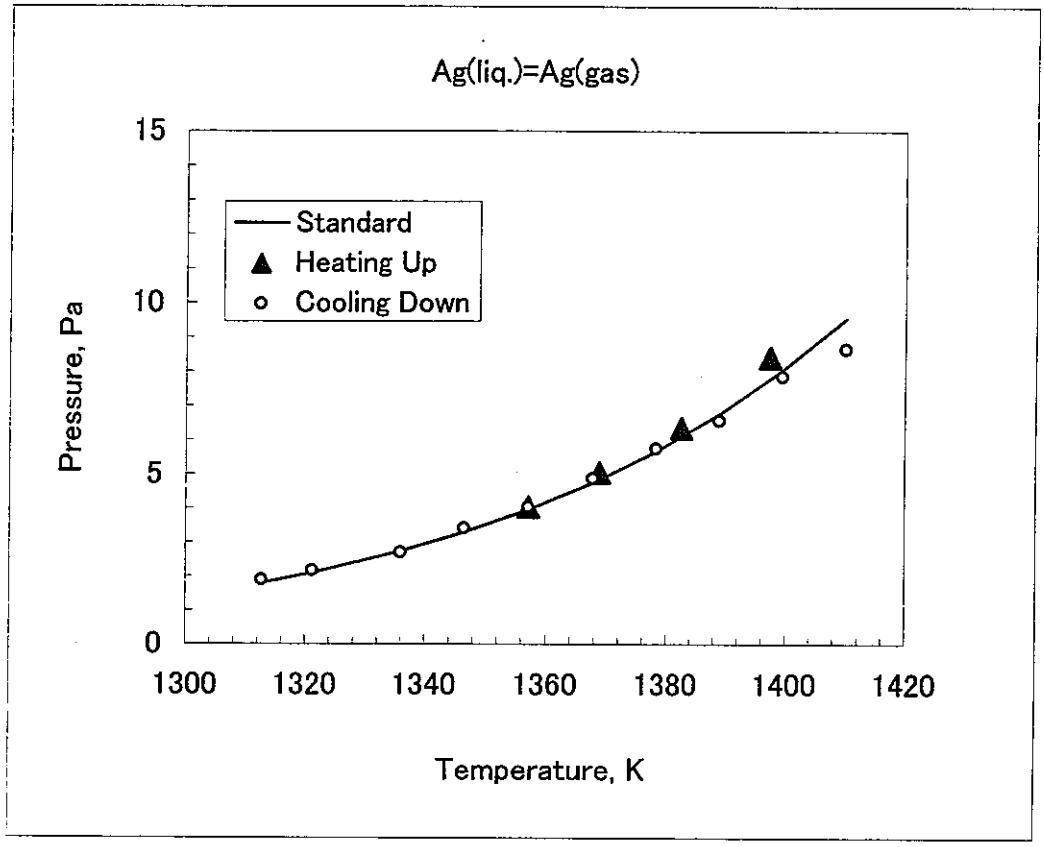

Fig. 32: Pressure calibration results by using silver as standard reference

From the above result, the proportional constant K in Eq. (1) was determined to be 3.42E+05 by the least-square method.

For lead, pressure calibration result is shown in Fug. 32. The equilibrium pressure of Pb(liq.)=Pb(gas) is reported as the following equation [Ref.6],

$$\lg(P/\text{bar}) = -10028/T - 0.92\,\lg(T) + 8.006 \qquad (10)$$

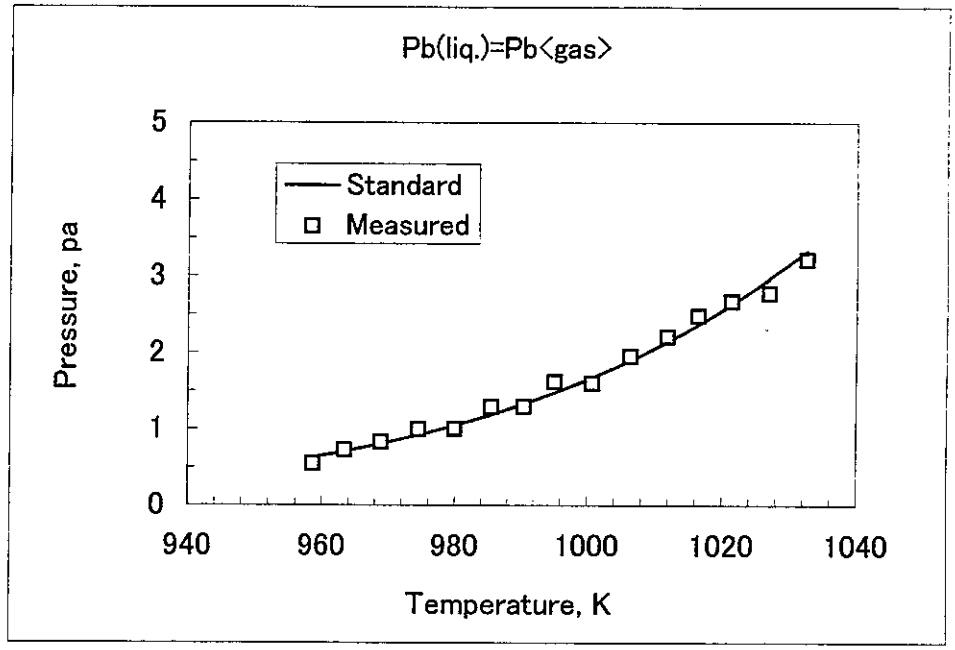

Fig. 33: Pressure calibration results by using lead as standard reference

From the above two independent measurements, the proportional constant Ks obtained are almost identical. The error is only about 1.6%.

Tab. 7: Pressure calibration result: Proportional constant Ks

	By Ag^{107}	By Pb^{208}	Average
Ks, $\times 10^5$	3.43	3.32	3.375±0.055

However, one should always keep in mind that the proportional constant K is not a universal constant at all. It definitely will change as long as one of the most important measurement conditions is changed, not only the parameters of the emission current, electron impact energy, but also the geometry of the heating system, shape or size of the K-cell, and so on...

Here are the measurement conditions required to use the proportional constant listed in Table 7.

Electron emission current (E.C.):	0.29 mA
Impact electron energy (E.E.) :	20 eV
Ion energy (I.E.):	5.5 eV
Extract Voltages (Ex. V.):	110 V
Geometrical position of the K-cell:	
Vertical position of the K-cell (Z-axis):	0. mm
Left (X-axis):	5.07 mm
Right (X-axis):	5.83 mm
Back (Y-axis):	5.08 mm
Front (Y-axis):	5.21 mm

If anything is changed and measurement cannot be done at the same condition as described above, one should use standard substance to calibrate it again the similar way as reported here.

Conclusions

The system adjustment and calibrations have been carried out for the vapor pressure measurement instrument. After various testes and conformation experiments, all the most important parameters of the Q-mass spectrometer were determined. The system was optimized for practical vapor pressure measurements. In the optimized condition, the proportional constant, *Ks*, of the system was obtained to be 337500±5500. So, the absolute partial vapor pressure of a vapor species can be calculated by using the following formula,

$$P(Pa) = K_s \times \frac{I \times T}{\alpha \times \beta \times \sigma}$$

where *Ks* is the proportional constant, *I* is the value of ion intensity measured from the Q-mass analyzer, *T* in Kelvin is the true temperature inside the K-cell, σ is the electron impact ionization cross section of the target ion in unit of 1E–16 cm^2, α is the isotope abundance of the target ion, β is the electron magnification factor in unit of one.

Acknowledgements

The authors would like to thank Dr. Jun-ichi Saito for his great efforts paid in the initial design of the system one year ago. His works made it possible for us to concentrate on system adjustment and modification directly. Special thanks are given to Prof. M. Yamawaki and Mr. M. Yasumoto, the Univ. of Tokyo, for their valuable comments to the system. Finally, we highly appreciate the leadership of Mr. Kazumi Aoto and assistances from other members of the Structure Safety Engineering Group.

References

(1) Klaus Hilpert, "Chemistry of Inorganic Vapors", Structure and Bonding 73, p97-198, Springer-verlag Berlin Heidelberg 1990.

(2) Ian Mills, etc., "Quantities, Units and Symbols in Physical Chemistry", p90-98, Black Scientific Publications, 1988.

(3) Jintao Huang, Doctoral Thesis, No. tt47282, Department of Quantum Engineering & System Science, the University of Tokyo, Sept. 30, 1997.

(4) H. P. Loock, L. M. Beaty and B. Simard, Phys. Rev. Vol. A 59, 1999, p873-875.

(5) Robert S. Freund, Robert C. Wetzel, Randy j. Shul and Todd R. Hayes, Phys. Rev., Vol. A 41, No.7, 1990, p3575-3595.

(6) I. Ansara, Thermodynamic Modeling and Materials data Engineering, J.P. Caliste, A. Truyoland and J.H.Westbrook Eds., Springer-Verlag Berlin 1998, p33-38.

(7) O. Knacke and O. Kubaschewski and K. Hesselmann, Thermochemical Propertites of Inorganic Substances, Springer-Verlag Berlin, Heidelberg 1991, p1 and p1536.